K. J. GURUBEL et al., Hybrid Intelligent Inverse Optimal Control for Methane …, *Chem. Biochem. Eng. Q.* **27** (2) 197–210 (2013)

197

Hybrid Intelligent Inverse Optimal Control for Methane Production in an Anaerobic Process

K. J. Gurubel,[a,*] F. Ornelas-Tellez,[b] E. N. Sanchez,[a] and S. Carlos-Hernandez[c]

[a]CINVESTAV, Unidad Guadalajara, Departamento de Control Automático,
Av. del bosque 1145, colonia el bajío, Zapopan, Jal., México 45019.

[b] División de Estudios de Posgrado, Facultad de Ingeniería Eléctrica, UMSNH,
F.J. Mujica SN, Ciudad Universitaria, Morelia, Mich., México 58030.

[c]Cinvestav, Unidad Saltillo, Grupo de Investigación en Recursos Naturales
y Energéticos, Carretera Saltillo-Monterrey Km. 13.5, Ramos Arizpe,
Coahuila, México 25900.

Anaerobic processes are very attractive because of their waste treatment properties and their capacity for transforming waste materials in order to generate methane, which can be used as a renewable energy source. A hybrid intelligent control strategy for an anaerobic process is proposed in this work; the structure of this strategy is as follows: a) a control law calculates dilution rate and bicarbonate addition in order to track a methane production reference trajectory; this control law is based on speed-gradient inverse optimal neural control, b) a nonlinear discrete-time recurrent high-order neural observer is used to estimate biomass concentration, substrate degradation and inorganic carbon, and c) a Takagi-Sugeno supervisor, which detects the process state, selects and applies the most adequate control action, allowing a smooth switching between open loop and closed loop. The applicability of the proposed scheme is illustrated via simulations considering a completely stirred tank reactor.

Key words:

Anaerobic process, methane production, hybrid intelligent control, neural observer, inverse optimal neural control, Takagi-Sugeno supervisor

Introduction

Motivated by the rapid growth of electricity demand, considering the depletion of fossil fuels, and due to increased environmental awareness, developed countries began to investigate the potential of renewable energy sources.[1–3] In recent years, with varying degrees of success, different renewable energy sources have been and continue to be studied for electric power generation, among them, geothermal, biomass, solar, wind, hydropower by micro-turbines and tidal waves.[4–6] Research on the optimization of energy generation in hybrid systems, which use different renewable sources, are discussed by Liang *et al.*[7] and Marwali *et al.*[8] Biomass is attractive as a potential energy resource, and it is an important fuel in several developing countries.[9] There are different reasons for biomass utilization as an energy source. One of them is that the amount of traditional petroleum sources for conventional fuels is not unlimited, while biomass is potentially renewable.[10] Another reason is that replacing fossil fuels with biomass would reduce the net carbon dioxide emissions that are contributing to the greenhouse warming of Earth.[11] Moreover, biomass fuels have a reasonable heat of combustion, and they usually have low sulfur, nitrogen and ash content as compared to many coals and oils.[12] Biomass may be converted into a variety of energy forms including heat (via burning), steam, electricity, hydrogen, ethanol, methanol, and methane.[13–16] Anaerobic digestion is a biological process by which organic matter (substrate) is degraded by anaerobic bacteria (biomass), in the absence of oxygen. Such degradation produces biogas, consisting primarily of methane (CH_4) and carbon dioxide (CO_2), and stable organic residues. Anaerobic digestion is a complex and sequential process which occurs in four basic stages: hydrolysis, acidogenesis, acetogenesis and methanogenesis.[17] Each stage has specific dynamics; hydrolysis, acidogenesis and acetogenesis are fast stages in comparison with methanogenesis, which is the slowest one; it imposes the dynamics of the process and is considered as the limiting stage. For this paper, the process is developed in a continuously stirred tank reactor (CSTR), with immobilized bacteria on a solid support. A variety of factors affect the rate of diges-

*Corresponding author: {kgurubel, sanchez}@gdl.cinvestav.mx

tion and biogas production, such as pH, temperature and overloads.[18] In addition, some variables and parameters are hard to measure due to economic or technical constraints. Then, estimation and control strategies are required in order to guarantee adequate performance.[19] In biological processes, there exist hardly measurable or nonmeasurable variables which are necessary for process control. Different biogas sensors have been developed in order to measure CH_4.[20–22] However, substrate and biomass measures are more restrictive. A discrete-time recurrent high-order neural observer (RHONO) for nonlinear systems, which model is assumed to be unknown is proposed by Alanis *et al.*[23] and Belmonte-Izquierdo *et al.*[24] This neural observer is based on a discrete-time recurrent high-order neural network (RHONN) trained with an extended Kalman filter (EKF)-based algorithm, using a parallel configuration. In this paper, the RHONO structure is modified in order to obtain a better estimation. The objective is to estimate biomass concentration, substrate degradation and inorganic carbon in the anaerobic process. The training of the RHONO is performed on-line. The variables are estimated from CH_4 and dioxide flow rates, which are commonly measured in this process. It is assumed that pH, YCH_4, YCO_2 and the process inputs are on-line measured. Neural networks are considered as good candidates for nonlinear systems applications, which deal with uncertainties, and are attractive due to their simpler implementation, robustness and the capacity to adjust their parameters on-line; additionally, the knowledge of the model is not strictly necessary.[25] In order to control the anaerobic process, a speed-gradient inverse optimal neural control is considered;[26] which is developed on the basis of the above mentioned neural observer. The controllers are designed to regulate bicarbonate in the reactor by two control actions: a base supplying ($b_{inc,k}$) and dilution rate ($D_{in,k}$) changes. Speed-gradient inverse optimal neural control is an adequate and novel algorithm in biological systems.[27] The aim of the inverse optimal control is to avoid the solution of the HJB (Hamilton-Jacobi-Bellman) equation,[28,29] diminishing implementation complexity.[30] A fuzzy supervisor is implemented in order to apply control actions to reject large disturbances on input substrate and to track a methane reference trajectory production. A Takagi-Sugeno supervisor[31,32] detects the process state, selects and applies the most adequate control action, allowing a smooth switching between open loop and closed loop. The process works in open loop in presence of small disturbances. For large disturbances, the supervisor allows the control actions to be applied avoiding washout; after that, the process returns to open loop operation. In general, the supervisor improves the

performances of the anaerobic process and is feasible for application in real processes, since the control scheme shows a good compromise between efficiency and complexity.

Mathematical model

A functional diagram of anaerobic digestion is proposed by Beteau[33] as shown in Fig. 1. Biomass is classified as: X_1, corresponding to hydrolytic, acidogenic and acetogenic bacteria, and X_2, which represents methanogenic bacteria. On the other hand, the organic load is classified in S_1, the components *equivalent glucose*, which model complex molecules and S_2, the components *equivalent acetate*, which represent the molecules directly transformed in acetic acid. This classification allows the process to be represented by a fast stage, which involves hydrolysis, acidogenesis and acetogenesis and a slow stage, which corresponds mainly to methanogenesis.
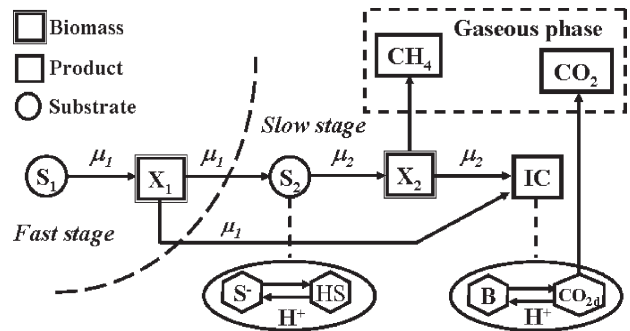

F i g . 1 – *Functional diagram of the anaerobic digestion*

Thus, a discrete-time nonlinear mathematical model of the process is deduced in Carlos-Hernandez *et al.*[17] On one side, the biological phenomena are modeled by ordinary differential equations (1), which represent the dynamic part of the process as:

$$X_{1,k+1} = X_{1,k} + (\mu_{1,k} - k_{d1})X_{1,k},$$

$$S_{1,k+1} = S_{1,k} - R_6\mu_{1,k}X_{1,k} + D_k(S_{1in,k} - S_{1,k}),$$

$$X_{2,k+1} = X_{2,k} + (\mu_{2,k} - k_{d2})X_{2,k},$$

$$S_{2,k+1} = S_{2,k} - R_3\mu_{2,k}X_{2,k} + R_4\mu_{1,k}X_{1,k} + \\ + D_k(S_{2in,k} - S_{2,k}), \quad (1)$$

$$IC_{k+1} = IC_k + R_2R_3\mu_{2,k}X_{2,k} + R_5\mu_{1,k}X_{1,k} - \\ - \lambda_k R_1 R_3 \mu_{2,k} X_{2,k} + D_k(IC_{in,k} - IC_k),$$

$$Z_{k+1} = Z_k + D_k(Z_{in,k} - Z_k),$$

where $\mu_{1,k}$ is the growth rate (Haldane type) of $X_{1,k}$ (h^{-1}) at step k, $\mu_{2,k}$ the growth rate (Haldane type) of

$X_{2,k}$ (h^{-1}), k_{d1} the death rate of $X_{1,k}$ (h^{-1}), k_{d2} the death rate of $X_{2,k}$ (h^{-1}), D_k the dilution rate (h^{-1}), $S_{1in,k}$ the fast degradable substrate input (mol L^{-1}), $S_{2in,k}$ the slow degradable substrate input (mol L^{-1}), IC inorganic carbon (mol L^{-1}), Z the total of cations (mol L^{-1}), $IC_{in,k}$ the inorganic carbon input (mol L^{-1}), $Z_{in,k}$ the input cations (mol L^{-1}), λ_k is a coefficient considering law of partial pressure for the dissolved CO_2 and $R_1, \ldots, R_6$ are the yield coefficients.

The growth rate for $X_{1,k}$ and $X_{2,k}$ are described by equations (2) and (3) respectively:

$$\mu_{1,k} = \frac{\mu_{1\,max} S_{1,k}}{k_{s1} + S_{1,k} + \dfrac{S_{1,k} HS}{k_{i1}}} \qquad (2)$$

$$\mu_{2,k} = \frac{\mu_{2\,max} S_{1,k}}{k_{s2} + HS + \dfrac{HS^2}{k_{i2}}} \qquad (3)$$

where μ_{1max} (h^{-1}) and μ_{2max} (h^{-1}) are the maximum growth rate for the $X_{1,k}$ and $X_{2,k}$ biomasses respectively, k_{S1} (mol L^{-1}) and k_{S2} (mol L^{-1}) are the growth saturation for the biomasses, k_{i1} (mol L^{-1}) and k_{i2} (mol L^{-1}) are the inhibition constants by substrate excess, HS is non ionized acetic acid (mol L^{-1}). and $S_{1,k}$ (mol L^{-1}) is slow stage substrate.

On the other side, the physical-chemical phenomena (acid-base equilibriums and material conservation) are modeled by algebraic equations (4).

$$HS + S^- - S_2 = 0,$$
$$H^+ S^- - K_a HS = 0,$$
$$H^+ B - K_b CO_{2d} = 0, \qquad (4)$$
$$B + CO_{2d} - IC = 0,$$
$$B + S^- - Z = 0,$$

where HS is non ionized acetic acid (mol L^{-1}), S^- ionized acetic acid (mol L^{-1}), H^+ ionized hydrogen (mol L^{-1}), B measured bicarbonate (mol L^{-1}), CO_{2d} dissolved carbon dioxide (mol L^{-1}), K_a is an acid-base equilibrium constant, K_b is an equilibrium constant between B and CO_{2d}.

Finally, the gaseous phase (CH_4 and CO_2) is considered as the process output:

$$Y_{CO_2,k} = \lambda_k R_2 R_3 \mu_{2,k} X_{2,k} \qquad (5)$$

$$X_{CH_4,k} = R_1 R_2 \mu_{2,k} X_{2,k} \qquad (6)$$

λ is a pressure partial coefficient for CO_2 defined as:

$$\lambda_k = \frac{CO_{2d}}{P_t K_h - CO_{2d}} \qquad (7)$$

where P_t is atmospheric pressure (Pa), K_h is a gases Henry constant (mol L^{-1} Pa^{-1}) and CO_{2d} defined as before. Biomass growth, substrate degradation and CO_2 are good indicators of CH_4 production[34] and biological activity inside the reactor. These variables can be used for monitoring the process and to design an inverse optimal neural control.

Discrete time neural observer

A nonlinear discrete-time recurrent high-order neural observer (RHONO) for unknown nonlinear systems in the presence of external disturbances and parameter uncertainties is described in Alanis *et al.*[23] This observer is based on a discrete-time recurrent high-order neural network (RHONN) trained with an extended Kalman filter (EKF) based algorithm. Let us consider the next nonlinear system, which is assumed to be observable:

$$x_{k+1} = F(x_k, u_k) + d_k,$$
$$y_k = h(x_k), \qquad (8)$$

where $x \in R^n$ is the state vector of the system, $u \in R^m$ is the input vector, $y \in R^p$ is the output vector, $h(x(k))$ is a nonlinear function of the system states, $d(w_k) \in R^n$ is a disturbance vector and $F(\cdot)$ is a smooth vector field and $F_i(\cdot)$ its entries; hence (8) can be also expressed component-wise as:

$$x_k = [x_{1,k} \ldots x_{i,k} \ldots x_{n,k}]^T,$$
$$d_k = [d_{1,k} \ldots d_{i,k} \ldots d_{n,k}]^T,$$
$$x_{i,k+1} = F_i(x_k, u_k) + d_{i,k}, \quad i = 1, \ldots, n, \qquad (9)$$
$$x_k = h(x_k).$$

For system (9), a *Luenberger-like* neural observer is proposed, with the following structure:

$$\hat{x}_k = [\hat{x}_{1,k} \ldots \hat{x}_{i,k} \ldots \hat{x}_{n,k}]^T,$$
$$\hat{x}_{i,k+1} = w_i^T z_i(\hat{x}_k, u_k) + g_{mi} e_k, \qquad (10)$$
$$\hat{y}_k = h(\hat{x}_k); \quad i = 1, \ldots, n,$$

with $g_{mi} \in R^p$, u_i is the external input vector to the NN and z_i is a function of states and inputs to each neuron; the weight vectors are updated on-line with a decoupled extended Kalman filter (EKF). The output error is defined by:

$$e_k = y_k - \hat{y}_k, \qquad (11)$$

and let us define the w_i^* estimate as w_i; then, the weights estimation $\tilde{w}_{i,k}$ and state observer $\tilde{x}_{i,k}$ errors are stated, respectively, as

$$\widetilde{w}_{i,k} = w_{i,k} - w_i^* \qquad (12)$$

$$\widetilde{x}_{i,k} = x_{i.k} - \hat{x}_{i,k}. \qquad (13)$$

For more details on the design and the stability analysis of this RHONO, we refer the reader to the results presented in Sanchez *et al.*[35]

In this paper, considering the RHONO advantages mentioned in section 1 and due to the requirement of nonmeasurable variables estimation for discrete-time speed gradient inverse optimal neural control, we propose the use of a discrete-time RHONO structure, which estimates the variables of the methanogenesis stage: biomass ($X_{2,k}$), substrate ($S_{2,k}$) and inorganic carbon (IC_k); the biomass is used in the supervisor structure; the substrate and the inorganic carbon are estimated for comparison (with real measures) in future researches. The observability property of this anaerobic digestion process is analyzed by Alcaraz-Gonzalez *et al.*[36] It is concluded that substrates ($S_{1,k}$ and $S_{2,k}$), biomasses ($X_{1,k}$ and $X_{2,k}$) and inorganic carbon (IC_k) are observable states. In Fig. 2, the proposed observer scheme is displayed and its formulation is shown by equations (14).
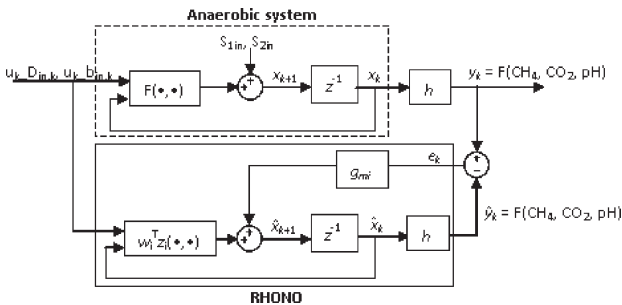

F i g. 2 – *Observer scheme*

where k is a real number representing a time sample, $x_{k+1} \in R^n$ is the state vector of the anaerobic system, $u_{k\_Din,k}$, $u_{k\_bin,k} \in R^m$ the inputs vector, $y_k \in R^p$ the output vector of the anaerobic system, $\hat{y}_k \in R^p$ the output vector estimated as a function of $\hat{x}_k$, CH_4, CO_2 and pH measurements, S_{1in}, $S_{2in} \in R^n$ substrates disturbances vector, e_k the output error, $F(\cdot,\cdot)$ and $w_i^T z_i(\cdot,\cdot)$ a smooth vector fields.

$$\hat{X}_{2,k+1} = w_{11}S(\hat{X}_{2,k}) + w_{12}S^2(\hat{X}_{2,k}) + w_{13}S(\hat{IC}_k) + \\ + w_{14}S^2(\hat{X}_{2,k})D_{in,k} + w_{15}S^2(\hat{X}_{2,k})b_{inc,k} + g_{m1}e_k,$$

$$\hat{S}_{2,k+1} = w_{21}S(\hat{S}_{2,k}) + w_{22}S^2(\hat{S}_{2,k}) + w_{23}S(\hat{IC}_k) + \\ + w_{24}S^2(\hat{S}_{2,k})D_{in,k} + w_{25}S^2(\hat{S}_{2,k})S_{2in,k} + g_{m2}e_k, \qquad (14)$$

$$\hat{IC}_{k+1} = w_{31}S(\hat{IC}_k) + w_{32}S^2(\hat{IC}_k) + w_{33}S(\hat{X}_{2,k}) + \\ + w_{34}S^2(\hat{IC}_k)D_{in,k} + w_{35}S^2(\hat{IC}_k)b_{inc,k} + g_{m3}e_k,$$

where w_{ij} is the respective on-line adapted weight vector; $\hat{X}_{2,k}$, $\hat{S}_{2,k}$ and $\hat{IC}_k$ are the estimated states; $S(\cdot)$ is the sigmoid function defined as $S(x) = \alpha \tanh(\beta x)$, $S^2(\cdot)$ is the square of the sigmoid function; (g_{m1}, g_{m2}, g_{m3}) are the Luenberger-like observer gains, e_k is the output error, $D_{in,k}$, $S_{2in,k}$ and $b_{inc,k}$ are defined as before.

EKF training algorithm

The Kalman filter (KF) provides an efficient computational solution to estimate the state of a linear dynamic system with additive state and output white noises.[35] For KF-based NN training, the network weights become the states to be estimated. In this case, the error between the NN output and the measured plant output can be considered as additive white noise. If, however, the model is nonlinear, the use of KF can be extended through a linearization procedure; the resulting filter is the well-known EKF. Since the NN mapping is nonlinear, an EKF-type is required. The training goal is to find the optimal weight values, which minimize the predictions error. In this work, an EKF-based training algorithm[37–40] described by (15) is used.

$$w_{i,k+1} = w_{i,k} + \eta_i K_{i,k} e_{i,k},$$

$$K_{i,k} = P_{i,k} H_{i,k} M_{i,k},$$

$$P_{i,k+1} = P_{i,k} - K_{i,k} H_{i,k}^T P_{i,k} + Q_{i,k}, \qquad (15)$$

$$M_{i,k} = [R_{i,k} + H_{i,k}^T P_{i,k} H_{i,k}]^{-1},$$

$$e_{i,k} = y_k - \hat{y}_k, \quad i = 1,\ldots,n$$

where $e_{i,k} \in R^P$ is the observation error, $P_{i,k} \in R^{Li}\text{x}Li$ is the prediction error covariance matrix at step k, $w_{i,k} \in R^{Li}$ is the weight (state) vector, L_i is the respective number of neural network weights, $y \in R^P$ is the plant output, $\hat{y}_k \in R^p$ is the NN output, η_i is the learning rate, $K_{i,k} \in R^{Li}\text{x}P$ is the Kalman gain matrix, $Q_{i,k} \in R^{Li}\text{x}Li$ is the NN weight estimation noise covariance matrix, $R_{i,k} \in R^P\text{x}P$ is the error noise covariance, and $H_{i,k} \in R^{Li}\text{x}P$ is the matrix for which each entry (H_{ij}) is the derivative of the *i-th* neural output with respect to *ij-th* NN weight, (w_{ij}). Where $i =1,\ldots, n$ and $j =1,\ldots, L_i$. Usually P_i, Q_i and R_i are initialized as diagonal matrices, with entries $P_{i,0}$, $Q_{i,0}$ and $R_{i,0}$ respectively. It is important to remark that $H_{i,k}$, $K_{i,k}$ and $P_{i,k}$ for the EKF are bounded.[41]

Speed-gradient inverse optimal neural control

As mentioned above, speed-gradient inverse optimal neural control is an adequate algorithm,

whose application in biological systems is novel.[27] The aim of the inverse optimal control consists of designing a stabilizing feedback control law, based on an a priori known control Lyapunov function (CLF) which ensures that the stabilizing control law optimizes a cost functional.[30] Let us consider the affine in the input discrete-time nonlinear system:

$$x_{k+1} = f(x_k) + g(x_k)u_k \qquad (16)$$

where $x \in R^n$ is the state of the system, $u \in R^m$ is the control input, $f(x)$ and $g(x)$ are smooth maps with $f(x) \in R^n$, $g(x) \in R^n \text{x} m$, $k \in Z^+ = \{0, 1, 2,...\}$. $f(0) = 0$ and $rank\ \{g(x)\}=m\ \forall x_k \neq 0$. In Ornelas *et al.*[30] the following cost functional is associated with system (16):

$$V(z_k) = \sum_{n=k}^{\infty}(l(z_n) + u_n^T R_C(z_n)u_n) \qquad (17)$$

where $z_k = x_k - x_{\delta,k}$ with $x_{\delta,k}$ as the desired trajectory for x_k; $z_k \in R^n$; $V(z_k): R^n \to R^+$; $l(z_k): R^n \to R^+$ is a positive semidefinite function and $R_C(z_k): R^n \to R^{mxm}$ is a real symmetric positive definite weighting matrix. The cost functional (17) is a performance measure.[42] The entries of $R_C(z_k)$ can be functions of the system state in order to vary the weighting on control efforts according to the state value.[42] Considering state feedback control, we assume that the full state x_k is available. Equation (17) can be rewritten as

$$V(z_k) = l(z_k) + u_k^T R_C(z_k)u_k +$$
$$+ \sum_{n=k+1}^{\infty}(l(z_n) + u_n^T R_C(z_n)u_n) = \qquad (18)$$
$$= l(z_k) + u_k^T R_C(z_k)u_k + V(z_{k+1})$$

where $V(z_{k+1})$ depends on both x_k and u_k by means of x_{k+1} in (16). In order to establish the conditions that the optimal control law must satisfy, we define the discrete-time Hamiltonian H[43] as

$$H(z_k,u_k)=l(z_k)+u_k^T R_C(z_k)u_k+V(z_{k+1})-V(z_k) \quad (19)$$

A necessary condition that the optimal control law u_k should satisfy is $\partial H/\partial u_k = 0$,[42] which is equivalent to calculate the gradient of (19) with respect to u_k, then

$$= 2R_C(z_k)u_k + \frac{\partial z_{k+1}}{\partial u_k}\frac{\partial V(z_{k+1})}{\partial z_{k+1}}$$

$$= 2R_C(z_k)u_k + \frac{\partial z_{k+1}}{\partial u_k}\frac{\partial V(z_{k+1})}{\partial z_{k+1}} \qquad (20)$$

$$= 2R_C(z_k)u_k + g^T(x_k)\frac{\partial z_{k+1}}{\partial u_k}\frac{\partial V(z_{k+1})}{\partial z_{k+1}}$$

Therefore, the optimal control law is formulated as

$$u_k^* = -\frac{1}{2}R^{-1}(z_k)g^T(x_k)\frac{\partial V(z_{k+1})}{\partial z_{k+1}}. \qquad (21)$$

For control law (21) in order to ensure trajectory tracking of system (16), a discrete-time CLF is proposed,[30] with the form:

$$V_c(z_k) = \frac{1}{2}z_k^T P_k z_k, \quad P_k = P_k^T > 0 \qquad (22)$$

This will be achieved by defining an appropiate matrix P_k; moreover it will be established that the control law (21) with (22), which is referred to as the inverse optimal control law, optimizes a cost functional of the form (17). Consequently, the control law takes the following form:

$$u_k^* = -\frac{1}{2}\left(R_C(z_k) + \frac{1}{2}g^T(z_k)P_k g(x_k)\right)^{-1} \times$$
$$\times g^T(x_k)P_k f(x_k,x_{\delta,k+1}) \qquad (23)$$

P_k and $R_C(z_k)$ are positive definite and symmetric matrices; thus, the existence of the inverse in (23) is assured. To compute P_k, which ensures stability of the system (16) with (23), the speed-gradient (SG) algorithm is used. Control law (23) at every time step depends on the matrix P_k. Let us define the matrix P_k at every time step k as:

$$P_k = p_k P_C \qquad (24)$$

where $P_C = P_C^T > 0$ is a given constant matrix and p_k is a scalar parameter to be adjusted by the SG algorithm.[26] Then, (23) is transformed into:

$$u_k^* = -\frac{p_k}{2}\left(R_C(z_k) + \frac{p_k}{2}g^T(x_k)P_C g(x_k)\right)^{-1} \times$$
$$\times g^T(x_k)P_C f(x_k,x_{\delta,k+1}) \qquad (25)$$

The dynamic variation of parameter p_k in (24) results in

$$p_{k+1} = p_k +$$
$$+ 8\gamma_{d,k}\frac{f^T(x_k)P_C g(x_k)R_C(z_k)^2 g^T(x_k)f(x_k)}{(2R_C(z_k) + p_k g^T(x_k)P_C g(x_k))^3} \qquad (26)$$

which is positive for all time step k if $p_0 > 0$. Therefore, positiveness for p_k is ensured and requirement $P_k = P_k^T > 0$ for (24) is guaranteed. With the control Lyapunov function as defined by (22) and $p_k = \bar{p}$ ($\bar{p}$ is a constant value when the SG algorithm converges) the control law is inverse optimal in the sense that it minimizes the cost functional (17),

which is proposed such that $l(z_k)$ ponders the states and $R_C(z_k)$ ponders the control.[26]

In order to apply the control law (25) to the anaerobic process, the following analysis is required, for which the proposed RHONO is presented as an affine system:

$$f_1(\hat{X}_{2,k}, \hat{IC}_k) = w_{11}S(\hat{X}_{2,k}) + w_{12}S^2(\hat{X}_{2,k}) +$$
$$+ w_{13}S(\hat{IC}_k) + g_{m1}e_k ,$$

$$f_2(\hat{S}_{2,k}, \hat{IC}_k) = w_{21}S(\hat{S}_{2,k}) + w_{22}S^2(\hat{S}_{2,k}) +$$
$$+ w_{23}S(\hat{IC}_k) + w_{25}S^2(\hat{S}_{2,k})S_{2in,k} + g_{m2}e_k , \quad (27)$$

$$f_3(\hat{X}_{2,k}, \hat{IC}_k) = w_{31}S(\hat{IC}_k) + w_{32}S^2(\hat{IC}_k) +$$
$$+ w_{33}S(\hat{X}_{2,k}) + g_{m3}e_k$$

$$G_{11}(\hat{X}_{2,k}) = w_{14}S^2(\hat{X}_{2,k}) \quad G_{12}(\hat{X}_{2,k}) = w_{15}S^2(\hat{X}_{2,k})$$

$$G_{21}(\hat{S}_{2,k}) = w_{24}S^2(\hat{S}_{2,k}) \quad G_{22}(\hat{S}_{2,k}) = 0 \quad (28)$$

$$G_{31}(\hat{IC}_k) = w_{34}S^2(\hat{IC}_k) \quad G_{32}(\hat{IC}_k) = w_{35}S^2(\hat{IC}_k)$$

$$g_1(\hat{x}_k) = \begin{bmatrix} G_{11} \\ G_{21} \\ G_{31} \end{bmatrix} \qquad g_2(\hat{x}_k) = \begin{bmatrix} G_{12} \\ G_{22} \\ G_{32} \end{bmatrix}$$

$$\qquad \qquad (29)$$

$$f_1(\hat{x}_k) = \begin{bmatrix} f_1 \\ f_2 \\ f_3 \end{bmatrix} \qquad f_{ref}(x_{\delta,k+1}) = \begin{bmatrix} X_{2ref} \\ S_{2ref} \\ IC_{ref} \end{bmatrix}$$

According to (25), the inverse optimal control law is formulated as

$$u^*_{k\_D_{in,k}} = -\frac{1}{2}\left(R_{C1}(z_k) + \frac{1}{2}g_1^T(\hat{x}_k)P_{1,k}g_1(\hat{x}_k)\right)^{-1} \times$$
$$\times g_1^T(\hat{x}_k)P_{1,k}f(\hat{x}_k, x_{\delta,k+1})$$

$$\qquad \qquad (30)$$

$$u^*_{k\_b_{inc,k}} = -\frac{1}{2}\left(R_{C2}(z_k) + \frac{1}{2}g_2^T(\hat{x}_k)P_{2,k}g_2(\hat{x}_k)\right)^{-1} \times$$
$$\times g_2^T(\hat{x}_k)P_{2,k}f(\hat{x}_k, x_{\delta,k+1})$$

where the positive definite matrix $P_k = p_k P_C$ is calculated by the SG algorithm, $R_C(z_k)$ is a constant matrix, $g(\hat{x}_k)$ and $f(\hat{x}_k)$ are matrices as in (27)-(28) and $f(\hat{x}_k, x_{\delta,k+1}) = f(\hat{x}_k) - f_{ref}(x_{\delta,k+1})$.

The tracking of a desired trajectory, defined in terms of the plant state $x_{i,k}$ formulated as (1) can be established as the following inequality:

$$\|x_{i,\delta} - x_{i,k}\| \le \|x_{i,k} - \hat{x}_{i,k}\| + \|x_{i,\delta} - \hat{x}_{i,k}\| \quad (31)$$

where $\|.\|$ stands for the Euclidean norm, $\hat{x}_{i,k}$ is the observed state, $x_i\delta$ is the desired trajectory signal,

which assume smooth and bounded. This proposition is possible based on the separation principle for discrete-time nonlinear system.[30] From (31), we establish the following requirements for the neural network tracking and control solution:

Requirement 1:

$$\lim_{t\to\infty}\|X_{i,k} - \hat{x}_{i,k}\| \le \zeta_i \quad (32)$$

with ζ_i a small positive constant.

Requirement 2:

$$\lim_{t\to\infty}\|X_{i,\delta} - \hat{x}_{i,k}\| \le \zeta_i \quad (33)$$

An on-line neural observer trained with extended Kalman filter based on (15) ensures (32),[44] while (33) is guaranteed by a discrete controller developed using the inverse optimal control technique.

Hybrid intelligent control scheme

Anaerobic digestion is able to work adequately without control for an interval of operating conditions and even in presence of small disturbances. However, for large disturbances, a control law is required in order to maintain process stability. Then, supervision of key variables is a very important task. The ODL/X_2 is the quantity of organic load that a unit of biomass can treat in a working day and is important regarding process stability.[17] It is defined as:

$$ODL/X_2 = D_{in,k}A_2S_{20}/\hat{X}_2 \quad (34)$$

where $D_{in,k}$ is the dilution rate (h^{-1}), A_2 a disturbance amplitude on the substrate input S_{2in} (mol L^{-1}), S_{20} the initial value of the substrate S_2 (mol L^{-1}) and is the estimated biomass X_2 (mol L^{-1}).

In the presence of a disturbance in S_{2in}, ODL/X_2 can abruptly increase up to a value, which exceeds the conditions of stability limits (critical value); therefore the process tends to washout, that means, the absence of active microorganisms and then the increase of nontreated substrate. If ODL/X_2 is above its critical value, then a control law must be applied in order to allow biomass growth, and hence, diminishing ODL/X_2 and stabilizing the system. In contrast, if the ODL/X_2 is under its critical value then the system can work in open loop. Depending on the ODL/X_2 value, commutation between operating modes (open loop, closed loop) is done by a Takagi-Sugeno fuzzy supervisor.[45] This commutation takes place progressively in order to avoid abrupt switching. The fuzzy set is defined as in Fig. 3.
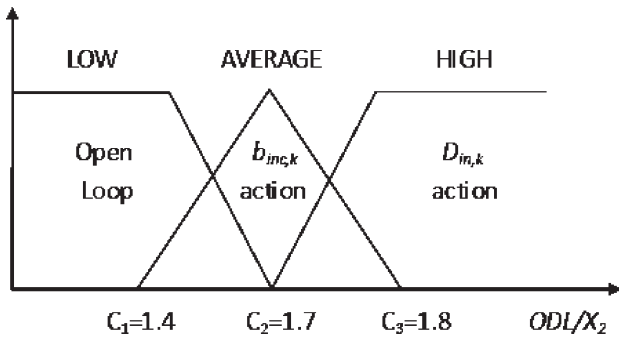
F i g 3　– *Fuzzyfication ODL/X_2*

The Takagi-Sugeno algorithm is used to define the supervisor. From empirical knowledge, each fuzzy set is associated with a control action; then three fuzzy inference rules are deduced:

If ODL/X_2 is LOW then u = open loop

If ODL/X_2 is AVERAGE then $u = b_{inc,k}$ action

If ODL/X_2 is HIGH then $u = D_{in,k}$ action

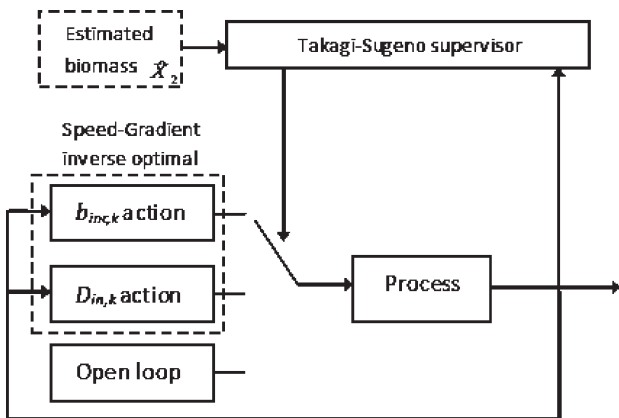The structure of the hybrid intelligent control is shown in Figure 4.

F i g . 4　– *Hybrid intelligent control scheme*

The main advantage of this control scheme is to combine different control actions in order to minimize their drawbacks and profit from their advantages: dilution rate ($D_{in,k}$) changes reject larger disturbances and supplying a base ($b_{inc,k}$) allows the process to track reference methane production. The operation mode in open loop works satisfactorily in the presence of small disturbances, which represents saving of energy. Consequently, the most adequate control action is applied in order to avoid washout.

Simulation results

The whole control strategy for the anaerobic process is implemented using Matlab™ and parameter values are presented in Tables 1, 2 and 3. The

T a b l e 1 – *Parameter values for anaerobic digestion model*

Kinetic parameters			Initial conditions		
Symbol	Value	Unit	Symbol	Value	Unit
μ_{1max}	0.205	h^{-1}	$X_{1,0}$	5.6836	mol L^{-1}
k_{s1}	0.26	mol L^{-1}	$S_{1,0}$	0.0537	mol L^{-1}
k_{i1}	16.333E-4	mol L^{-1}	$X_{2,0}$	0.0068	mol L^{-1}
μ_{2max}	0.017	h^{-1}	$S_{2,0}$	0.0037	mol L^{-1}
k_{s2}	2.18E-5	mol L^{-1}	IC_0	0.0817	mol L^{-1}
k_{i2}	8.22E-3	mol L^{-1}	Z_0	0.0551	mol L^{-1}
Equation parameters			D_{in}	0.1	h^{-1}
Symbol	Value	Unit	SI_{in}	10	mol L^{-1}
k_{d1}	0.035	h^{-1}	$S2_{in}$	0.07	mol L^{-1}
k_{d2}	0.0085	h^{-1}	IC_{in}	0.0051	mol L^{-1}
R_1	0.99		Z_{in}	0.0051	mol L^{-1}
R_2	0.99				
R_3	345				
R_4	0.0666				
R_5	0.0005				
R_6	5				
K_a	1.7E-5	mol L^{-1}			
K_b	1.7E-7	mol L^{-1}			
Kh	0.065	mol L^{-1} Pa^{-1}			
P_t	1	Pa			

T a b l e 2 – *Parameter values for neural observer*

Symbol	Value	Unit	Symbol	Value	Unit
$w_{11}, w_{12}, w_{13}, w_{14}, w_{15}$	0.0068	mol L^{-1}	g_{m1}	0.12	
$w_{21}, w_{22}, w_{23}, w_{24}, w_{25}, w_{26}$	0.0037	mol L^{-1}	g_{m2}	0.09	
$w_{31}, w_{32}, w_{33}, w_{34}, w_{35}$	0.0817	mol L^{-1}	g_{m3}	0.09	
$P_{1,0}$	1500		η_1	2	
$P_{2,0}$	1000		η_2	1	
$P_{3,0}$	1500		η_3	10	
$Q_{1,0}$	1.5		$\hat{X}_{21}$	0.0102	mol L^{-1}
$Q_{2,0}$	1.5		$\hat{S}_{21}$	0.0046	mol L^{-1}
$Q_{3,0}$	0.2		$\hat{IC}$	0.1223	mol L^{-1}
$R_{1,0}$	150				
$R_{2,0}$	150				
$R_{3,0}$	1.5				

observer is initialized at random values to verify the estimation convergence. In order to test the observer sensitivity to input changes, a disturbance of

T a b l e 3 – *Controller parameters*

Symbol	Value	Unit	Symbol	Value	Unit
R_{C1}	0.6		R_{C2}	0.4	
$P_{C1,11}$	2.8E4		$P_{C2,11}$	729	
$P_{C1,12}$	0.25E4		$P_{C2,12}$	437	
$P_{C1,13}$	0.23E4		$P_{C2,13}$	291	
$P_{C1,21}$	0.25E4		$P_{C2,21}$	437	
$P_{C1,22}$	0.05E4		$P_{C2,22}$	729	
$P_{C1,23}$	0.04E4		$P_{C2,23}$	629	
$P_{C1,31}$	0.23E4		$P_{C2,31}$	291	
$P_{C1,32}$	0.04E4		$P_{C2,32}$	629	
$P_{C1,33}$	0.05E4		$P_{C2,33}$	729	
g_{S1}	1600		g_{S2}	500	

50 % $S2in$ increase in the input substrate is incepted at $t = 200$ hours. The performance of the proposed RHONO and the input disturbance substrate is illustrated in Fig. 5.

It is clear that the biomass, substrate, and inorganic carbon are well estimated. Additionally, robustness of the proposed RHONO is tested in the presence of a 80 % disturbance in $200 < t < 500$, different initial conditions and parameters variation in the biomasses growth. A 10 % negative variation in the maximum rate growth of the hydrolytic, acidogenic and acetogenic bacteria (μ_{1max}) and a 10 % positive variation in the maximum rate growth of the methanogenic bacteria (μ_{2max}). Parameter values are in Table 4 and the performance of the proposed RHONO is illustrated in Fig. 6.

System states are well estimated and the robustness of the proposed RHONO to parameters variations is verified. Thus, the proposed neural observer is a good alternative to estimate those important states of the considered anaerobic process. Model and observer validation are found in Belmonte et al.[46]

As mentioned in section 5, the inverse optimal neural control algorithm requires reference trajectories. In a previous work[48] anaerobic system was controlled in the presence of disturbances with a PI L/A controller which avoided inhibition; the process presented a suitable behavior which was reflected in trajectories for methane production. Therefore these trajectories represent an adequate dynamic behavior of the anaerobic process for growth biomass and methane production in the presence of disturbances and are smooth. Hence, they are selected as reference trajectories for inverse optimal neural control. The hybrid control scheme is tested in the presence of a 100 % distur-
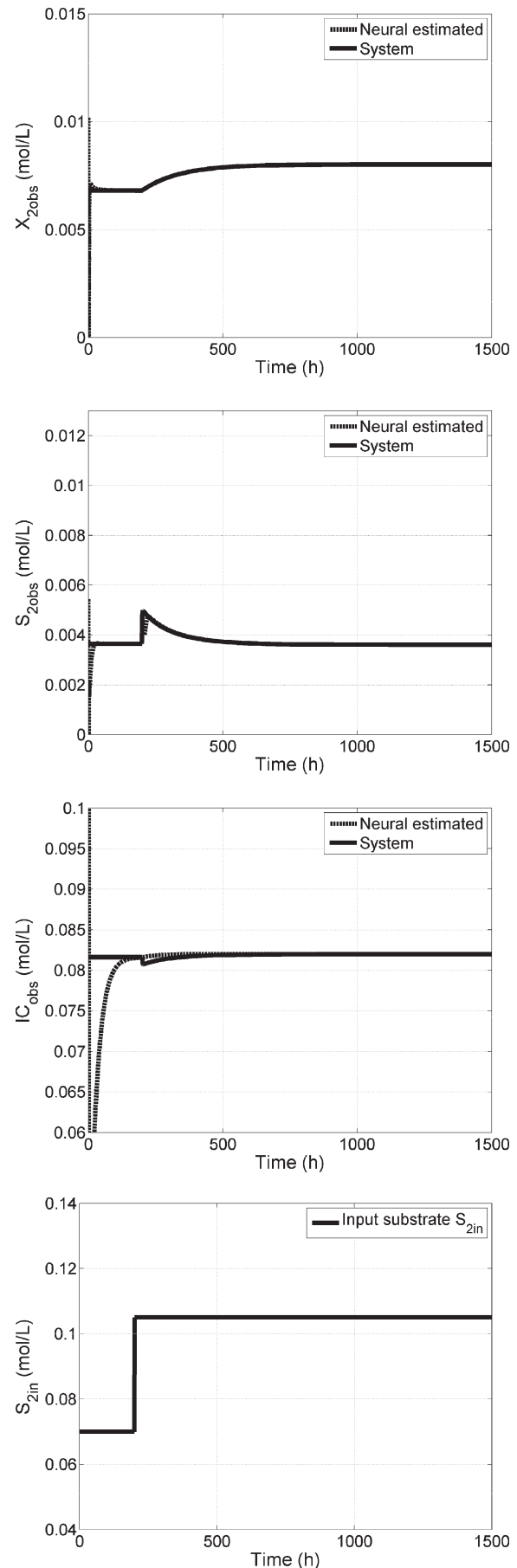

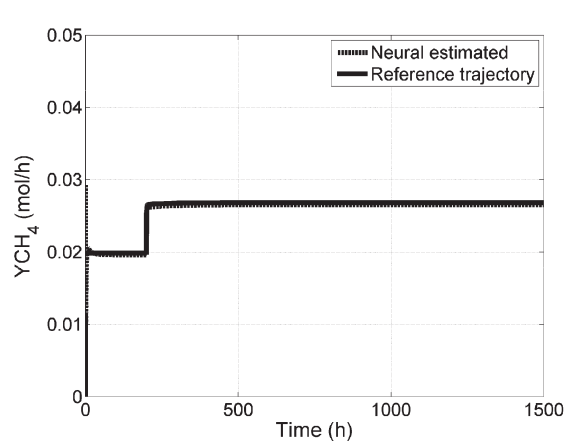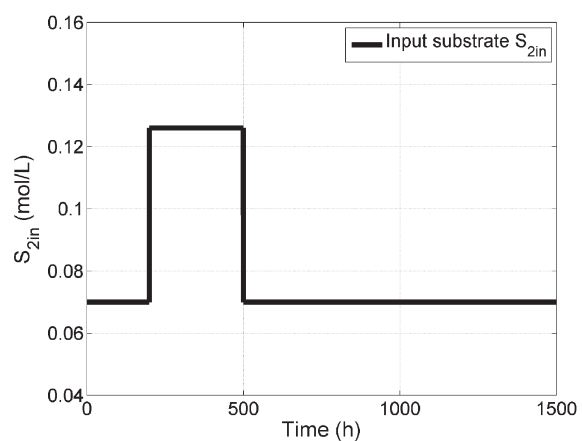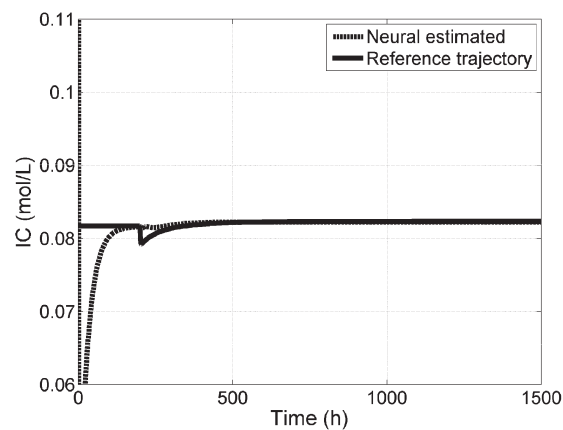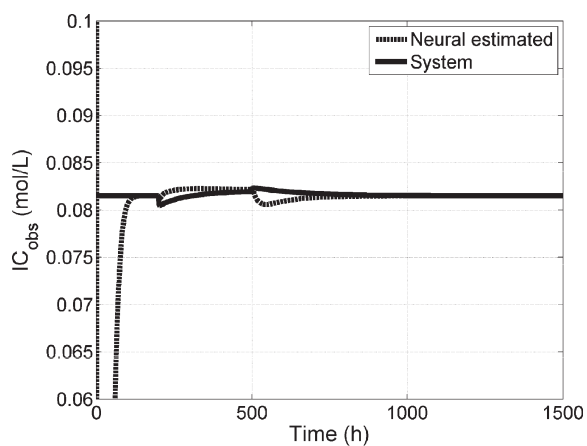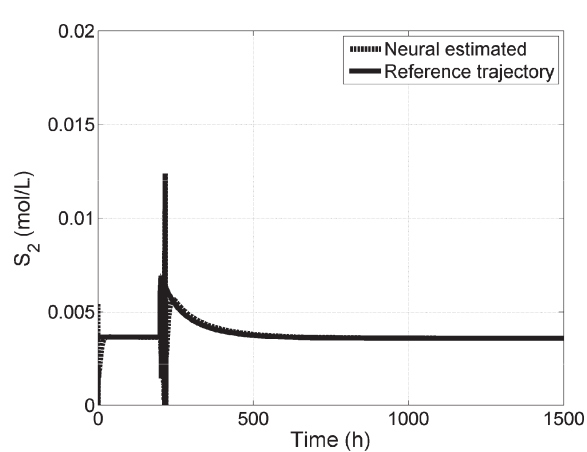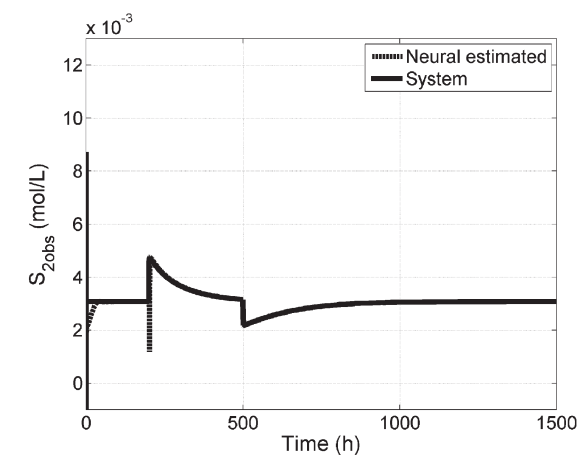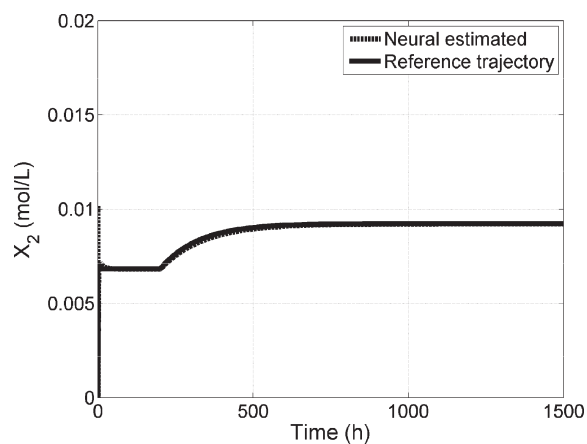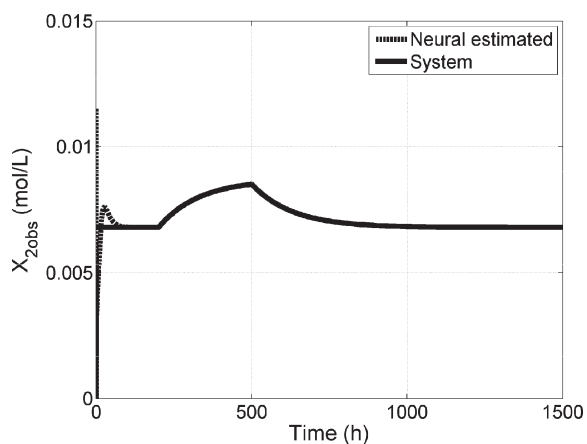F i g. 5 – *State estimation for a 50 % disturbance*

F i g. 6 – *State estimation for parameters variation*

F i g. 7 – *Trajectories tracking states for a 100 % disturbance*

bance on S_{2in}, incepted at $t=200$ hours. Trajectories tracking for states and YCH_4 are illustrated below.

When the disturbance is introduced in the input substrate, an adequate control law must be applied in order to allow biomass growth, and hence, diminishing ODL/X_2 and stabilizing the system. As can be seen the process operates in open loop because disturbance is small; this is because ODL/X_2 belongs to the associated fuzzy set corresponding to open loop (Fig. 3). This situation implies that the anaerobic digestion process is able to work adequately without control in the presence of this small disturbance. Thus, trajectory tracking for the states is achieved as illustrated in Fig. 7 and the error approaches zero in steady state. The YCH_4 is calculated with equation (6), which is based on the system observed states. As can be seen, the reference is reached; Fig. 8 displays the inputs $b_{inc,k}$ and $D_{in,k}$.
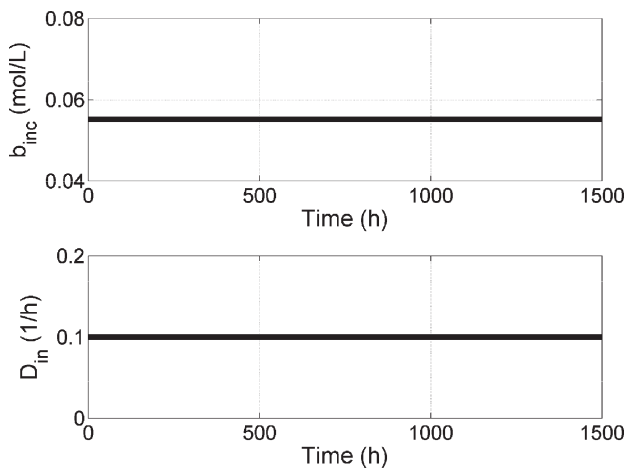

F i g . 8 – *Input signals for a 100 % disturbance*

The proposed hybrid control scheme is also tested introducing a 150 % disturbance in S_{2in} incepted at $t=200$ hours, as illustrated in Fig. 9.

For this case, the supervisor operates in closed loop because the disturbance is large and closed loop control is required. During disturbance, ODL/X_2 increases its value until reaching a level corresponding to HIGH fuzzy set. Therefore the system goes to closed loop operation mode applying control action $D_{in,k}$. During the evolution process, ODL/X_2 diminishes its level and starts to belong to HALF fuzzy set. Thus control action $b_{inc,k}$ is applied and the control action $D_{in,k}$ is stopped. Finally, ODL/X_2 diminishes its value until belonging to the fuzzy set associated to open loop. This situation implies that the disturbance has been rejected completely. Under these last conditions, supervisor stops the action $b_{inc,k}$ and the process returns to its operation in open loop. Thus, trajectory references for the states are reached with error approaching
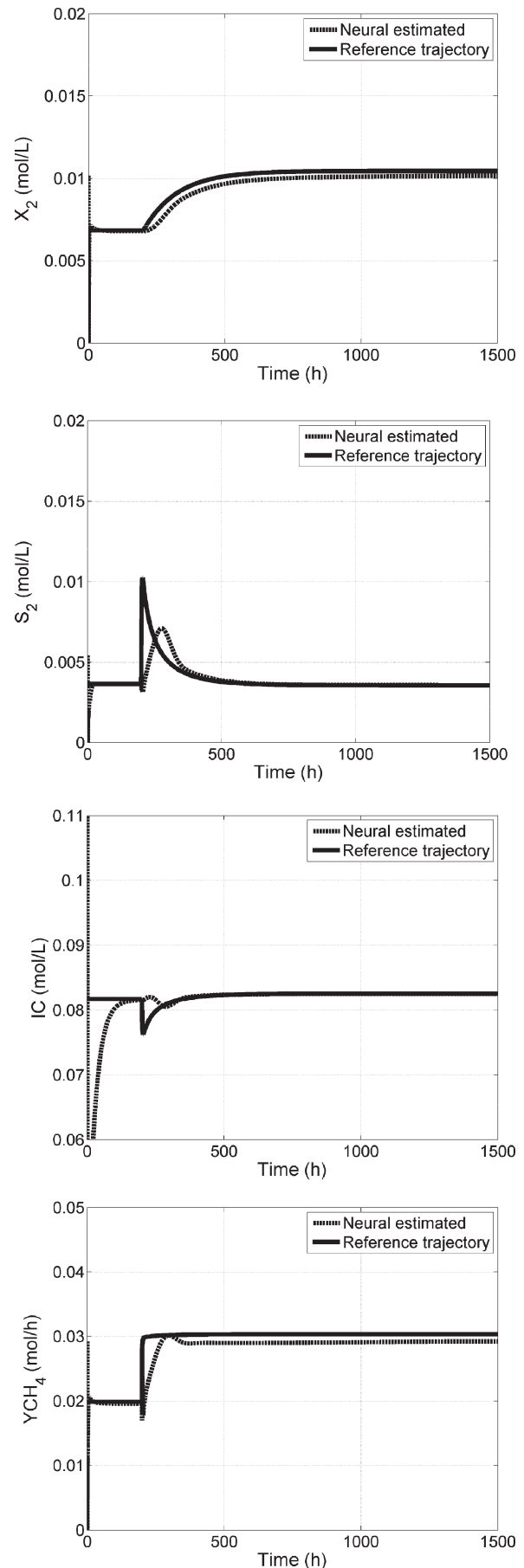

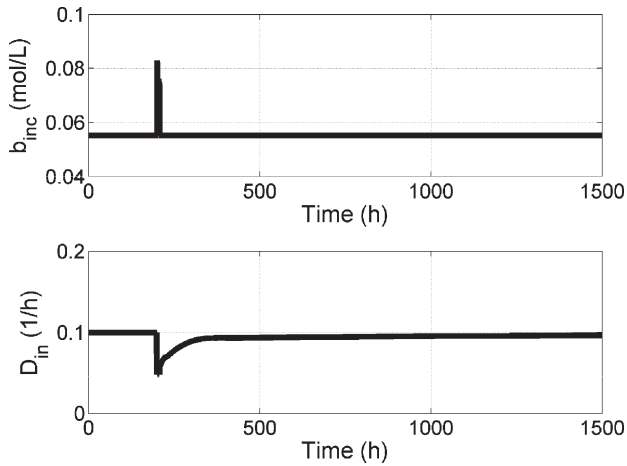F i g . 9 – *Trajectories tracking states for a 150 % disturbance*

F i g . 1 0 − *Control signals for a 150 % disturbance*

zero at steady state as illustrated in Fig. 9. Also, YCH_4 reaches its reference and the corresponding error approaches zero at steady state. Fig. 10 displays the control signals $b_{inc,k}$ and $D_{in,k}$.

The proposed hybrid control scheme is also tested introducing a 200 % disturbance in S_{2in} incepted at t=200 hours, as illustrated below.

As can be seen in Fig. 11, the proposed scheme detects a large disturbance and applies the adequate control action until the disturbance is rejected. Thus trajectory tracking is efficient and the error approaches zero at steady state. YCH_4 reference is reached with a small error at steady state as is illustrated in Fig. 11. Fig. 12 displays the control signals $b_{inc,k}$ and $D_{in,k}$. System operation is ensured due to the control strategy applied, even though a large disturbance is incepted. For the case of disturbances larger than 200 % in S_{2in}, the oscillation induced by the observer prevents the supervisor from controlling the process. Therefore, the system tends to washout; a critical value exists for which the supervisor cannot control the bio-process due to the magnitude of the disturbances.
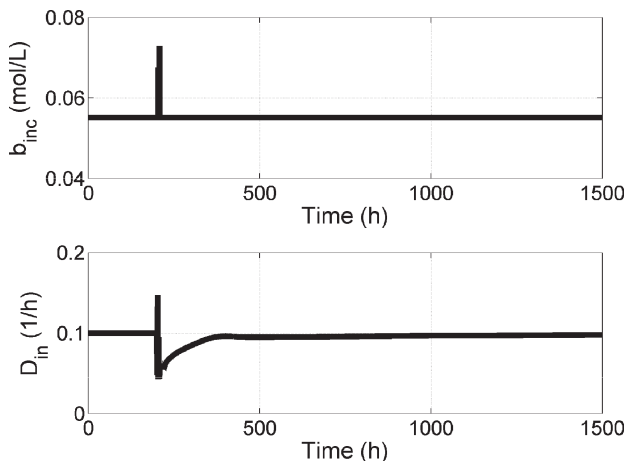

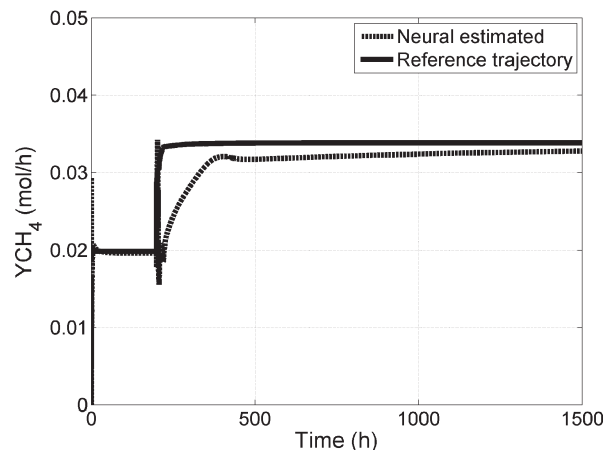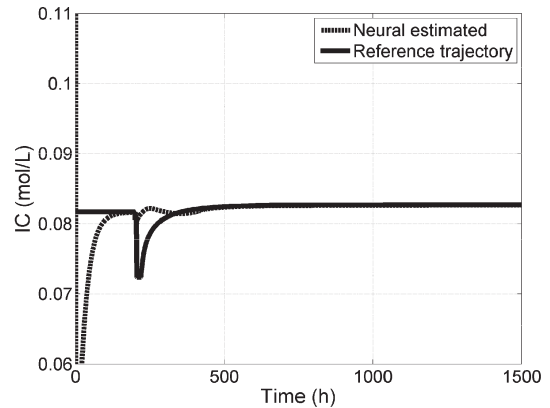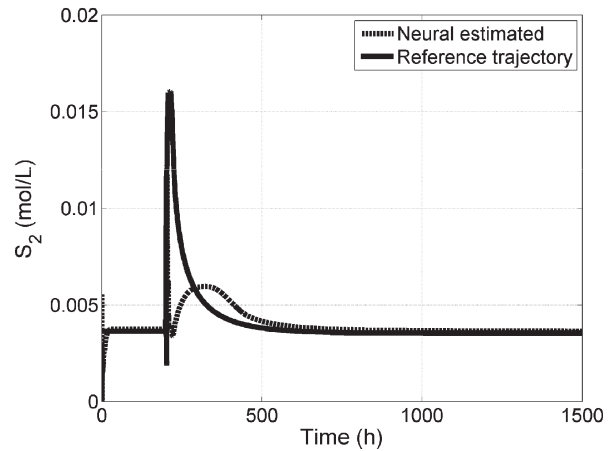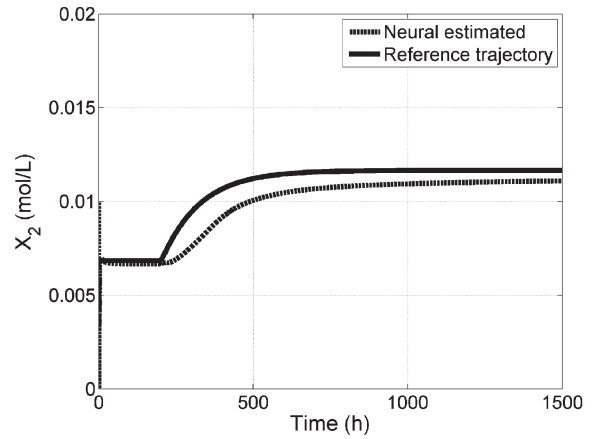F i g . 1 2 − *Control signals for a 200 % disturbance*

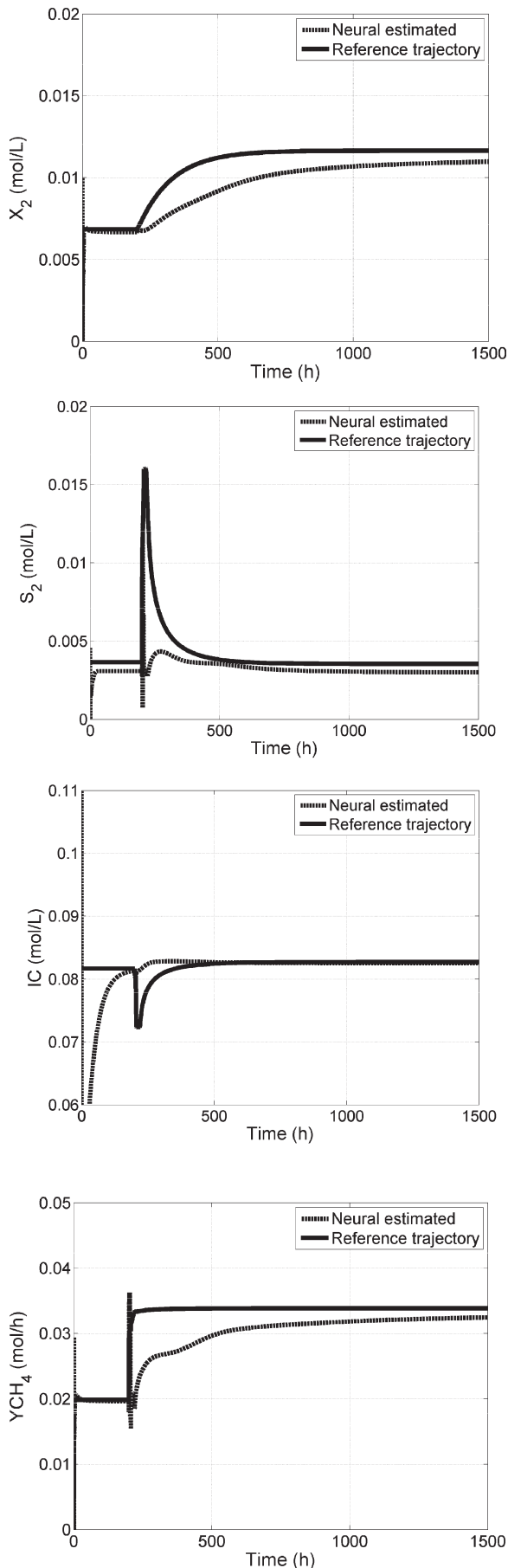F i g . 1 1 − *Trajectories tracking for a 200 % disturbance*

F i g . 1 3 — *Trajectories tracking for parameter variation*

Finally, controller tolerance to change of the system parameters is tested; such variation is incepted as a disturbance in the bacteria concentration, μ_{1max} and μ_{2max} as presented in Table 4, and a disturbance in the input substrate of 200 % S_{2in} increase incepted at t=200 h as in Fig. 11. Performance of the system is illustrated in Fig. 13.

T a b l e 4 — *Parameter values variation*

Symbol	Value	Unit
$\hat{X}_{2,1}$	0.0116	mol L^{-1}
$\hat{S}_{2,1}$	0.0052	mol L^{-1}
$\hat{IC}$	0.1386	mol L^{-1}
μ_{1max}	0.1845	h^{-1}
μ_{2max}	0.0188	h^{-1}

As illustrated in Fig. 13, the closed loop performance presents a transient state error which is due to parameters variation in rate growths that affect directly the kinetic; the control scheme acts in order to track the trajectory which is achieved at steady state with a small error. The control trajectories are illustrated in Fig. 14.
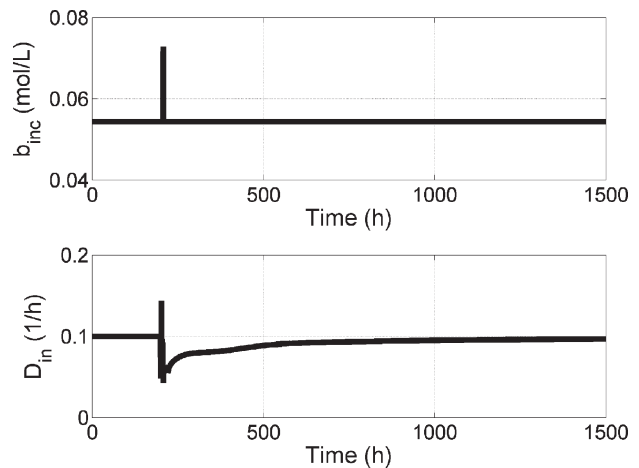
F i g . 1 4 — *Control signals for parameter variation*

System states are well estimated and the robustness of the proposed RHONO to parameters variations is verified. Thus, the proposed neural observer is a good alternative to estimate those important states of the considered anaerobic process. Model and observer validation are found in Belmonte *et al.*[46] Fuzzy PI control for the same process is discussed in Belmonte *et al.*[46] There, the goal was not to track specific trajectories, but to avoid washout. PID control is unsuitable for time-varying trajectory tracking. Due to these two facts, comparison with these control schemes is not included in this paper.

Conclusions

In this paper, a hybrid intelligent control scheme for an anaerobic wastewater treatment process is proposed in order to produce methane and avoid washout. A nonlinear discrete-time recurrent high-order neural observer (RHONO) is used to estimate the biomass concentration, substrate degradation, and inorganic carbon; then this observer is transformed into an affine mathematical model with the aim of applying speed-gradient inverse optimal neural control. Once this model is obtained, an inverse control law, based on it, is developed. The fuzzy supervisor detects biological activity inside the tank reactor, on the basis of estimated biomass, and applies a control action. The goal is to force the system to track desired reference, which is achieved; simulation results show how the hybrid intelligent control is able to stabilize the methane production along desired trajectories in the presence of disturbances, and avoiding washout. Thus, control action fulfills the objectives of rejecting disturbances, and of obtaining a high efficiency of the process, which is reflected in a good production of biogas. This research will be pursued in order to evaluate the application in real-time of the proposed control scheme to an anaerobic prototype process.

List of symbols

YCH_4 – methane production, mol h^{-1}

YCO_2 – carbon dioxide production, mol h^{-1}

D_{in} – dilution rate, h^{-1}

b_{inc} – provided bicarbonate, mol L^{-1}

X_1 – hydrolytic, acidogenic and acetogenic bacteria, mol L^{-1}

X_2 – methanogenic bacteria, mol L^{-1}

S_1 – fast degradable substrate, mol L^{-1}

S_2 – slow degradable substrate, mol L^{-1}

IC – inorganic carbon, mol L^{-1}

S_1in – fast degradable substrate input, mol L^{-1}

S_{2in} – slow degradable substrate input, mol L^{-1}

IC_{in} – inorganic carbon input, mol L^{-1}

Z_{in} – input cations

λ – pressure partial coefficient

R_i – yield coefficients

HS – non ionized acetic acid, mol L^{-1}

H^+ – ionized hydrogen, mol L^{-1}

B – measured bicarbonate, mol L^{-1}

CO_{2d} – dissolved carbon dioxide, mol L^{-1}

K_a – acid-base equilibrium constant

K_b – equilibrium constant between B and CO_{2d}

$\hat{X}_2$ – biomass estimated, mol L^{-1}

$\hat{IC}$ – inorganic carbon estimated, mol L^{-1}

$\hat{S}_2$ – Substrate estimated, mol L^{-1}

e_k – output error, mol h^{-1}

$e_{i,k}$ – observation error, mol h^{-1}

R^P – espacio euclidiano de dimensión P

X_{k+1} – discrete state of the system

$V(.,.)$ – Lyapunov function

$x_{\delta,k}$ – desired trajectory

P_k – positive definite symmetric matrix gain

u_k – control law

J – cost function

ODL/X_2 – quantity of organic load treated by biomass unit by day, mol L^{-1} h^{-1}

A_2 – disturbance amplitude, mol L^{-1}

Abbreviations

TS – Takagi-sugeno

CSTR – continued stirred tank reactor

NN – neural network

RHONO – recurrent high-order neural observer

RHONN – recurrent high-order neural network

KFE – Kalman extended filter

SG – speed-gradient

References

1. *Erdinc,O., Uzunoglu, M.*, Renew. Ustain. Energy Rev. **16** (2012) 1412–1425.

2. *Georgilakis, P. S., Katsigiannis, Y. A.*, Renew. Energy **34** (2009) 65–70.

3. *Zeng, J., Wu, J., Gao, L., LI, M.*, An agent-based approach to renewable energy management in eco-building. IEEE International Conference on Sustainable Energy Technologies, 46–50, 2008.

4. *Kalantar, M., Mousavi G., S.M.*, Appl. Energy **87** (2010) 3051–3064.

5. *Mousavi G., S.M.*, Int. J. Elec. Power **43** (2012) 1144–1154.

6. *Nikkhajoei, H., Iravani, R.*, Electromagnetic transients of a micro-turbine based distributed generation system. International Conference on Power Systems Transients (IPST'05) Vol. 77, pp 1475–1482, in Montreal, Canada, 2007.

7. *Liang, R. H., Liao, J.H.*, IEEE Trans. Power Syst. **22** (2007) 1665–1674.

8. *Marwali, M. K. C., Haili, M., Shahidehpour, S. M., Abdul Rahman, K. H.*, IEEE Trans. Power Syst. **13** (1998) 1057–1062.

9. *Xuan, J., Leung, M. K.H., Leung, D. Y.C., Ni, M.*, Renew. Sustain. Energy Rev. **13** (2009) 1301–1313.

10. *Wang, L., Weller, C. L., Jones, D. D., Hanna, M. A.*, Biomass Bioenergy **32** (2008) 573–581.

11. *Hu, X., Lu, G.*, Int. J. Hydrogen Energy **35** (2010) 7169–7176.

12. *Zhang, L., Xu, C., Champagne, P.*, Energy Convers. Manage. **51** (2010) 969–982.

13. *Williams, R. H., Larson, E. D., Katofsky, R. E., Chen, J.*, Energy Sustainable Dev. **1** (1995) 18–34.

14. *Hamelinck, C. N., Faaij, A. P.C.*, J. Power Sources **111** (2002) 1–22.

15. *Clausen, L. R., Houbak, N., Elmegaard, B.*, Energy **35** (2010) 2338–2347.

16. *Mahishi, M. R., Goswami, D.Y.*, Int. J. Hydrogen Energy **32** (2007) 3831–3840.

17. *Carlos-Hernandez, S., Mallet, G., Beteau, J. F.*, Modelling and analysis of the anaerobic digestion process, 2nd Symposium on System, Structure and control, pp 311–316, Oaxaca, Mexico, 2004.

18. *Chen, Y., Cheng, J. J., Creamer, K. S.*, Bioresour. Technol. **99** (2007) 4044–4064.

19. *Simeonov, I. S., Kalchev, B. L., Christov, N. D.*, Parameter and State Estimation of an Anaerobic Digestion Model in Laboratory and Pilot-Scale Conditions, 18th IFAC World Congress, Vol. 18, Milano , Italy, 2011.

20. *Smith, S. A., Stöckle, C. O.*, Bioresour. Technol. **99** (2008) 8537–8539.

21. *Cadena Pereda, R.O., Rivera Muñ<255>oz, E.M.*, Herrera Ruiz, G., Sens. Actuators, B **147** (2010) 10–14.

22. *Ward, A. J., Bruni, E., Lykkegaard, M. K., Feilberg, A., Adamsen, A. P. S., Jensen, A. P., Poulsen, A. K.*, Bioresour. Technol. **102** (2011) 4098–4103.

23. *Alanis,A: Y. Sanchez, E. N., Loukianov, A. G., Perez, M. A.*, IEEE Trans. Neural Networks **22** (2011) 497–505.

24. *Belmonte-Izquierdo, R., Carlos-Hernandez, S., Sanchez, E. N.*, Int. J. Neural Syst. **20** (2010) 75–86.

25. *Ricalde L. J., Sanchez, E. N.*, Inverse optimal nonlinear high order recurrent neural observer, International Joint Conference on Neural Networks IJCNN 05, Vol. 1, pp 361–365, Montreal, Canada, 2005.

26. *Ornelas-Tellz, F., Sanchez, E. N., Loukianov, A. G.*, Navarro-Lopez, E. M., Speed-Gradient Inverse Optimal control for Discrete-Time Nonlinear Systems, 50th IEEE Conference on Decision and Control and European Control Conference (IEEE CDC-ECC), pp 290–295, Orlando, Florida, 2011.

27. *Leon, B. S., Alanis, A. Y., Sanchez, E. N., Ornelas-Tellez, F. & Ruiz-Velazquez, E.*, Inverse Optimal Trajectory Tracking for Discrete Time Nonlinear Positive Systems. Proceedings of 50th IEEE Conference on Decision and Control and European Control Conference (IEEE CDC-ECC), pp 1048–1053, Orlando, Florida, 2011.

28. *Sepulchre, R., Jankovic, M., Kokotovic, P. V.*, Constructive Nonlinear Control, pp 71–103, Springer-Verlag, New York, USA, 1997.

29. *Krstic, M., Deng, H.*, Stabilization of Nonlinear Uncertain Systems, pp 55–94, Springer-Verlag, New York, USA, 1998.

30. *Ornelas-Tellez, F., Sanchez, E. N., Loukianov, A. G.*, Decentralized inverse optimal neural control for trajectory tracking, Proceedings of the Annual Conference of Mexican Association of Automatic Control (AMCA), Puerto Vallarta, Jalisco, 2010.

31. *Takagi, T., Sugeno, M.*, IEEE Trans. Syst. Man Cybern. **15** (1985) 116.

32. *Tanaka, K., Wang, W. O.*, Fuzzy control systems design and analysis: a linear matrix inequality approach, pp 83–96, First ed., Wiley-Interscience, New York, 2001.

33. *Beteau, J. F.*, An industrial wastewater treatment bioprocess modelling and control, Ph. D. Thesis, INPG, France, 1992.

34. *Segers, R.*, Biogeochemistry **41** (1998) 23–51.

35. *Sanchez, E. N., Alanis, A. Y., Loukianov, A. G.*, Discrete Time High Order Neural Control Trained with Kalman Filtering, pp 45–57, Springer-Verlag, Germany, 2008.

36. *Alcaraz-Gonzalez, V., Gonzalez- Alvarez, V.*, Robust nonlinear observers for Bioprocesses: Application to wastewater treatment (Book Chapter in Selected Topics in Dynamics and Control of Chemical and Biological Processes), Springer-Verlag, pp 119–164, Berlin, Germany, 2007.

37. *Sanchez, E. N., Alanis, A. Y., Chen, G. R.*, Dynamics of Continuous, Discrete and Impulsive Systems Series B **13** (2006) 1–17.

38. *Jeong-Gwan, K., Su-Yong, A., Se-Young, O.*, Modified Neural Network aided EKF based SLAM for improving an accuracy of the feature map, , pp 1–7, Barcelona, 2010.

39. *Iltis, R.A.*, An EKF-based algorithm for PN code tracking in the presence of narrowband interference and multipath, Military Communications Conference, Conference Record, A New Era. IEEE 1990, Vol.3, pp 975–979, Monterey, CA, 1990.

40. *Ling, S.H., Leung, F.H.F., Lam, H.K., Yim-Shu L., Tam, P.K.S.*, IEEE Trans. Ind. Electron. **50** (2003) 793–799.

41. *Song, Y., Grizzle, J. W.*, JMSEC **5** (1995) 59–78.

42. *Kirk, D. E.*, Optimal Control Theory: An introduction. Prentice-Hall, NJ, USA, 1970.

43. *Haddad, W. M., Fausz, J. L., Chellaboina, V., Abdallah, C. T.*, J. Franklin Ins. **335** (1998) 827–839.

44. *Alanis, A. Y.*, Discrete-time Neural Control: Application to Induction Motors. PhD thesis. Centro de Investigación y Estudios Avanzados del IPN. Guadalajara, México, 2007.

45. *Ashoori, A., Moshiri, B., Khaki-Sedigh, A., Bakhtiari, M. R.*, J. Process Control **19** (2009) 1162–1173.

46. *Belmonte-Izquierdo, R.*, Estimación de Estado y Control Inteligente de Procesos Anaeróbicos de Tratamiento de Aguas Residuales, M.S. dissertation, Centro de Investigación y Estudios Avanzados del IPN., Guadalajara, México, 2009.